Journal of Hazardous Materials 185 (2011) 1124–1130

Contents lists available at ScienceDirect

Journal of Hazardous Materials

journal homepage: www.elsevier.com/locate/jhazmat

Application of bifunctional magnetic adsorbent to adsorb metal cations and anionic dyes in aqueous solution

Ya-Fen Lin [a], Hua-Wei Chen [b], Poh-Sun Chien [c], Chyow-San Chiou [c,*], Cheng-Chung Liu [c]

[a] Department of Chemical and Materials Engineering, National I-Lan University, I-Lan 260, Taiwan
[b] Department of Cosmetic Application & Management, St. Mary's Medicine Nursing and Management College, I-Lan, Taiwan
[c] Department of Environmental Engineering, National I-Lan University, 1, Sec. 1, Shen-Lung Road, I-Lan, 260, Taiwan

ARTICLE INFO

Article history:
Received 21 June 2010
Received in revised form 6 October 2010
Accepted 7 October 2010
Available online 14 October 2010

Keywords:
Magnetic adsorbent
SiO_2
Amine
Copper ion
RB5

ABSTRACT

A magnetic adsorbent, amine-functionalized silica magnetite ($NH_2/SiO_2/Fe_3O_4$), has been synthesized to behave as an anionic or cationic adsorbent by adjusting the pH value of the aqueous solution to make amino groups protonic or neutral. $NH_2/SiO_2/Fe_3O_4$ were used to adsorb copper ions (metal cation) and Reactive Black 5 (RB5, anionic dye) in an aqueous solution in a batch system, and the maximum adsorption were found to occur at pH 5.5 and 3.0, respectively. The adsorption equilibrium data were all fitted the Langmuir isotherm equation reasonably well, with a maximum adsorption capacity of 10.41 mg g^{-1} for copper ions and of 217 mg g^{-1} for RB5. A pseudo-second-order model also could best describe the adsorption kinetics, and the derived activation energy for copper ions and RB5 were 26.92 kJ mol^{-1} and 12.06 kJ mol^{-1}, respectively. The optimum conditions to desorb cationic and anionic adsorbates from $NH_2/SiO_2/Fe_3O_4$ were provided by a solution with 0.1 M HNO_3 for copper ions and with 0.05 M NaOH for RB5.

1. Introduction

The removal of heavy metal pollutants and azo dyes from wastewater has become an important issue because of their adverse effects on human health and the environment [1,2]. Traditional metal-ion treatment processes include chemical precipitation, ion exchange, electrolysis, reverse osmosis, adsorption, etc. Among these treatment methods, adsorption is considered to be an economical and efficient method for the treatment of metal-ion-contaminated wastewater [3]. Azo dyes are the most widely used commercial reactive dyes in dyeing processes, with a worldwide production of more than 4×10^5 tons per year [4]. During the manufacture process, approximately 10 wt% of the dye is lost [5]; this loss contributes to the total organic concentration of the effluent [6]. It has been shown that neither simple chemical nor biological treatment can achieve the desired decoloration and depletion of dye organic matter [5]. Therefore, the adsorption process is a suitable treatment method for the removal of dyes from wastewater [7,8].

Nowadays, most adsorbents developed for the removal of heavy metal ions and azo dyes rely on the interaction of the target compounds with the functional groups that are present on the surfaces of the adsorbents. The functional groups thus play an important role in determining the effectiveness, capacity, selectivity, and reusability of these adsorbents [9–12]. Adsorbents with amino groups have bifunctional properties that enable them to adsorb cationic and anionic target compounds with different pH values in aqueous solutions. Neutral nitrogen of amine group with a lone pair electrons have been found to be one of the most efficient functional groups for the removal of heavy metal ions [13–15], and protonic amino groups with a cationic charge can adsorb anionic pollutants by means of electrostatic attraction [16]. Various adsorbents with amine functional groups have been developed from natural biopolymers [17] or from synthetic polymers that are subsequently immobilized by the amine groups [18–21].

An innovative technology that has gained increasing attention involves solid–liquid phase separation and employs adsorbents with magnetic properties. Magnetic separation is now widely used in the fields of medicine, diagnostics, molecular biology, [22], bioinorganic chemistry, and catalysis [23,24]. Furthermore, the method of magnetic separation is beneficial to the environment because it does not produce contaminants such as flocculants [25]. Conventional magnetic adsorbents are generally commercial carriers made of magnetite particles modified with polymer [26] or organosilane [27], in which suitable functional groups are present on the adsorbent surface.

In the present study, a magnetic adsorbent made of magnetite with amino groups was developed to adsorb cations and anions; it was synthesized by the surface modification of Fe_3O_4 with SiO_2 and N-[3-(trimethoxysilyl)propyl]-ethylenediamine (TPED) containing amino functional groups. The pH effect, adsorption isotherm, adsorption kinetic, and recycling efficiency of this mag-

* Corresponding author. Tel.: +886 3 9357400x752; fax: +886 3 9359674.
E-mail address: cschiou@niu.edu.tw (C.-S. Chiou).

0304-3894/$ – see front matter © 2010 Published by Elsevier B.V.
doi:10.1016/j.jhazmat.2010.10.022

netic adsorbent were examined using copper ions and anionic azo dye (Reactive Black 5, RB5) as the model contaminants.

2. Materials and methods

2.1. Materials

Magnetite (Fe_3O_4, particle size <5 μm), Reactive Black 5 (RB5, its molecule structure is shown in Fig. 1) and sodium silicate were purchased from Sigma–Aldrich (St. Louis, MO, USA). N-[3-(trimethoxysilyl)propyl]- ethylenediamine, (TPED, $C_8H_{22}N_2O_3Si$), $Cu(NO_3)_2{\cdot}3H_2O$, and 4-nitrobenzaldehyde of high quality were purchased from Acros Organics (Belgium, USA) and used without any further purification. All other chemicals were of the reagent grade and were supplied by several suppliers.

2.2. Instruments

The functional groups of the synthesized adsorbents were confirmed using an FTIR spectrometer (Spectrum 100, PerkinElmer, USA). The specific surface area and pore diameter of the adsorbents were measured by the BET method using a particle size analyzer (ASAP 2000C, Micromeritics, USA). The magnetic behavior was analyzed using a vibrating sample magnetometer (VSM, Lake Shore 7407, Lake Shore, USA). The crystal lattice structure of the material was determined by XRD (Theta Probe, Thermo Scientific, UK). The concentration of metal ions in the solution was analyzed using a flame atomic absorption spectropotometer (AA932, GBC, Australia). The absorbance intensity of RB5 at the maximum visible absorbance wavelength ($A_{\lambda_{max}}$ at 595 nm) was measured using a spectrophotometer (Lambda 25, PerkinElmer, USA) and used to estimate the adsorption efficiency.

2.3. Synthesis of adsorbents

2.3.1. Silica-coated magnetite (SiO_2/Fe_3O_4)

A total of 1.08 L of an aqueous solution containing 20 g of magnetite (Fe_3O_4) particles was held in a 2-L beaker at 90 °C; its pH was maintained at 9.5 with 0.1 N NaOH, while it was being stirred by a mechanic stirrer. An appropriate amount of sodium silicate was dissolved in 100 mL of deionized water, and the resulting solution was mixed with the above aqueous solution of magnetite. The pH of this mixture was adjusted to 6 by using 5 N H_2SO_4, and the mixture was then maintained at 90 °C for 30 min under mechanical stirring [28]. Silica coating was applied by the aggregation of silicic acid monomer to form a gel by titration of the silicate solution with sulfuric acid [29]. Finally, the reacted magnetite were collected by applying external magnetic force and washed several times with deionized water until the pH of the water collected after washing the adsorbents became ~7. The prepared SiO_2/Fe_3O_4 was then dried at 105 °C for 8 h and stored in desiccators until further use in the following experiments.

2.3.2. Amine-modified silica magnetite ($NH_2/SiO_2/Fe_3O_4$)

Ten grams of the prepared SiO_2/Fe_3O_4 was reacted with N-[3-(trimethoxysilyl)-propyl]ethylenediamine in 500 mL of refluxing toluene under N_2 for 24 h. The resulting adsorbent was filtrated and washed by soxlet extraction with ethanol, and then these synthetic adsorbents was followed by drying at 60 °C in vacuum. The dry adsorbent was stored in a sealed bottle for further use.

2.4. Adsorption experiments

Adsorption of Cu^{2+} and RB5 from aqueous solutions was investigated in batch experiments. Effects of pH (2.0–12.0), kinetic experiments (0–5 h), adsorption isotherm (initial concentration 25–125 mg L^{-1} for Cu^{2+}, and 500–1000 mg L^{-1} for RB5), and thermodynamic studies (298–328 K) on adsorption were studied. All the adsorption isotherm experiments were carried out at 298 K, in which pH was maintained at a constant value during the whole reaction time, the adsorbent concentration was kept constant at 0.5 g in a 50-mL solution, the equilibrium time was considered as 24 h. After adsorption reached the equilibrium, the adsorbent was separated via an external magnetic field. The concentrations of Cu^{2+} ions and RB5 in the aqueous solution were analyzed using flame atomic absorption and visible absorption, respectively.

2.5. Desorption experiments

The experiments for desorption efficiency were carried out with HNO_3 or NaOH solutions in the concentration range of 0.01–2 M. A 0.5 g amount of the $NH_2/SiO_2/Fe_3O_4$ adsorbent adsorbed with copper ions or RB5 were placed into 100 mL of a HNO_3 or NaOH solution with thermostatic shaking and the desorption was allowed for a time period up to 24 h. The desorption efficiency (DE) was determined from the following equation:

$$\mathrm{DE} = \frac{C \times V}{q \times m} \times 100\%,$$

where C (mg L^{-1}) is the concentration of copper ions or RB5 in the desorption solution, V is the volume of the desorption solution, q (mg g^{-1}) is the amount of copper ions or RB5 adsorbed on the adsorbents before desorption experiment, and m (g) is the amount of the adsorbent used in the desorption experiments.

3. Results and discussion

3.1.1. Characterization of magnetic adsorbent

3.1.1.1. FTIR

The FTIR spectra of Fe_3O_4, SiO_2/Fe_3O_4, and the prepared magnetic amine adsorbent ($NH_2/SiO_2/Fe_3O_4$) are shown in Fig. 2. The figure exhibits two basic characteristic peaks of these three adsorbents at about 3300 cm^{-1} (O–H stretching) and 550 cm^{-1} (Fe–O vibration), which were attributed to the presence of FeOH in Fe_3O_4 [26]. The peaks at 1100 cm^{-1} were attributed to the Si–O–Si bond stretching of SiO_2/Fe_3O_4 and $NH_2/SiO_2/Fe_3O_4$ [30,31]. This result confirms that SiO_2 was successfully coated on Fe_3O_4. Further, in Fig. 2, the peaks of $NH_2/SiO_2/Fe_3O_4$ are located at 1496 cm^{-1} (C–H stretching) and 1643 cm^{-1} (N–H bending); these peaks indicated that TPED had been bonded with the surface of SiO_2/Fe_3O_4. Amine compound also possesses a characteristic peak around 3300 cm^{-1} (N–H stretching) in an IR spectrum, but this peak was interfered from O–H stretching absorbance. In addition, the characteristic peaks of C–H stretching and N–H bending for the synthesized $NH_2/SiO_2/Fe_3O_4$ were too weak to be observed clearly. Therefore,

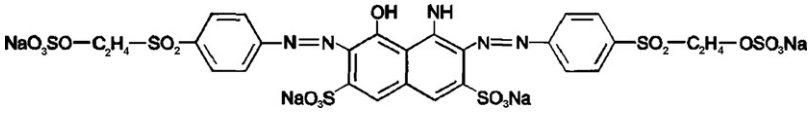

Fig. 1. The molecular structure of RB5 with molecular formula of $C_{26}H_{21}N_5O_{19}S_6Na_4$.

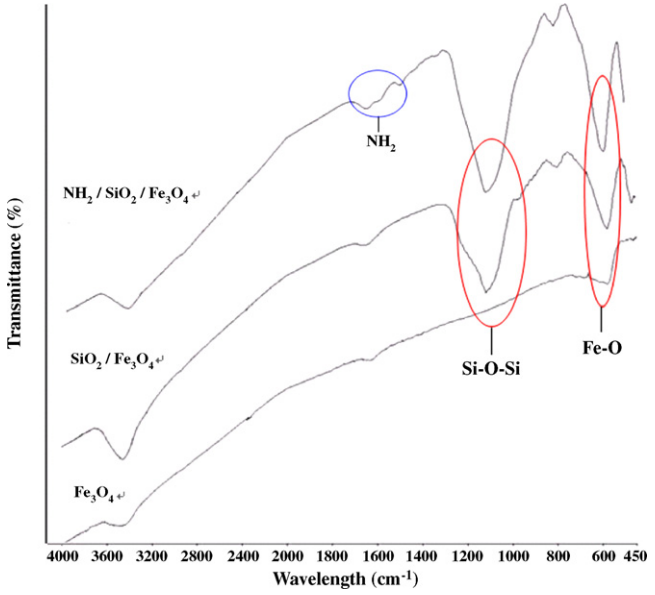

Fig. 2. FTIR spectra of Fe_3O_4, SiO_2/Fe_3O_4, and $NH_2/SiO_2/Fe_3O_4$.

another analytical method, UV absorbance, was employed to prove that the amine group had bonded on the surface of SiO_2/Fe_3O_4.

3.1.1.2. UV absorbance

The amine groups anchored on the support surface could be determined by a UV colorimetric method that involved their reaction with a UV-sensitive reagent (4-nitrobenzaldehyde) [32]. This reaction between amine and aldehyde groups under anhydrous conditions generates an imine group that may be hydrolyzed back to the precursors in a known volume of water to produce 4-nitrobenzaldehyde whose absorbance (282 nm) can be measured by UV spectroscopy. The number of hydrolyzed aldehyde molecules is proportional to the number of imine molecules present. Fig. 3 shows the results of colorimetric analyses performed on Fe_3O_4, SiO_2/Fe_3O_4, and $NH_2/SiO_2/Fe_3O_4$. It is clear that the UV absorbance at a wavelength of 282 nm in the case of $NH_2/SiO_2/Fe_3O_4$, containing an amine group, was larger than that in the case of Fe_3O_4 and SiO_2/Fe_3O_4. The UV absorbances of Fe_3O_4 and SiO_2/Fe_3O_4, without an amine group, were almost zero. These results also confirmed that the surface of the synthesized $NH_2/SiO_2/Fe_3O_4$ had been modified with amine group.

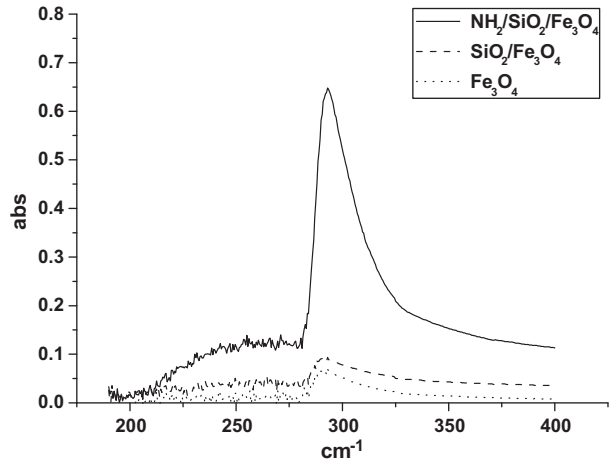

Fig. 3. The results of UV colorimetric analyses of amine groups with 4-nitrobenzaldehyde performed on Fe_3O_4, SiO_2/Fe_3O_4, and $NH_2/SiO_2/Fe_3O_4$. UV absorbance at wavelength 282 nm.

Table 1
The Brunauer–Emmett–Teller surface area of Fe_3O_4, SiO_2/Fe_3O_4, and $NH_2/SiO_2/Fe_3O_4$.

Magnetic catalyst	Surface area ($m^2\ g^{-1}$)
Fe_3O_4	18.06
SiO_2/Fe_3O_4	114.02
$NH_2/SiO_2/Fe_3O_4$	72.89

3.1.1.3. BET, XRD, VSM

BET surface area measurements indicated that compared to the Fe_3O_4 core, the surface area of SiO_2/Fe_3O_4 significantly increased from 18.06 $m^2\ g^{-1}$ to 114.02 $m^2\ g^{-1}$ (Table 1). The SiO_2 film coated on the Fe_3O_4 surface with sodium silicate underwent polymerization at a suitable solution pH value owing to the silicate [29], and the resulting SiO_2 polymer wrapped the core (Fe_3O_4). When the SiO_2-coated Fe_3O_4 substrate was dried, the porosity of the surface increased, thereby increasing the surface area. As shown in Table 1, when SiO_2/Fe_3O_4 was modified with the amine group, the BET surface area decreased to 72.89 $m^2\ g^{-1}$. This decrease in the surface area may be attributed to the possibility that the SiO_2 pore was partially covered by the modified amino compound (TPED).

According to the database of Joint Committee on Powder Diffraction Standards (JCPDS), the XRD pattern of a standard Fe_3O_4 crystal with spinel structure has six characteristic peaks at $2\theta = 30.1°$, 35.5°, 43.1°, 53.4°, 57.0°, and 62.6° that are attributed to the (2 2 0), (3 1 1), (4 0 0), (4 2 2), (5 1 1), and (4 4 0) phases of Fe_3O_4, respectively. It is apparent that as shown in Fig. 4, the analysis results of the starting material Fe_3O_4, SiO_2/Fe_3O_4, and $NH_2/SiO_2/Fe_3O_4$ fitted the pattern exhibited by standard magnetite. Therefore, it can be concluded that the magnetite modified with SiO_2 and TPED is also of spinel structure and that the modification does not cause a phase change in Fe_3O_4. Furthermore, since the SiO_2 coating and TPED were amorphous, new peaks attributable to these groups could not be detected in the XRD analysis.

The magnetic properties of the $NH_2/SiO_2/Fe_3O_4$ and Fe_3O_4 cores were measured by VSM and are shown in Fig. 5. The mass saturation magnetization (M_s) of Fe_3O_4 was found to be 61.8 emu g^{-1}, which is in good agreement with the value in literature [33]. The plots shown in Fig. 5 exhibited a change in M_s of the particles after the incorporation of a NH_2/SiO_2 shell. A decrease in M_s from 61.8 emu g^{-1} to 57.2 emu g^{-1} was observed in the case of $NH_2/SiO_2/Fe_3O_4$. This decrease was ascribed to the contribution of the nonmagnetic NH_2/SiO_2 shell to the total mass of the particles. This observation is similar to that made in another study, wherein the attached gold

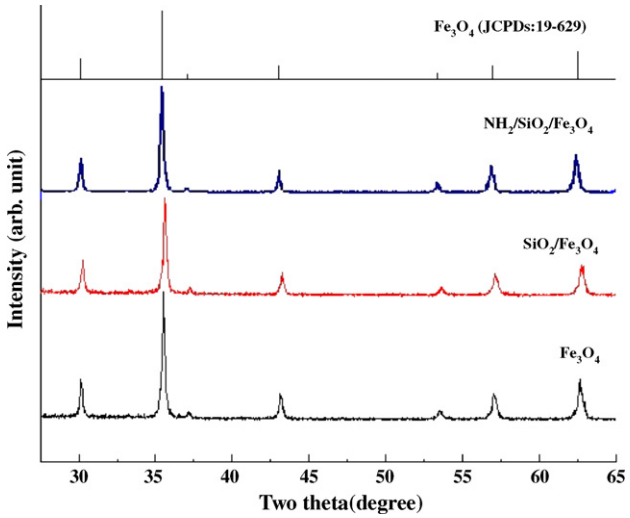

Fig. 4. The XRD spectra of Fe_3O_4, SiO_2/Fe_3O_4, and $NH_2/SiO_2/Fe_3O_4$.

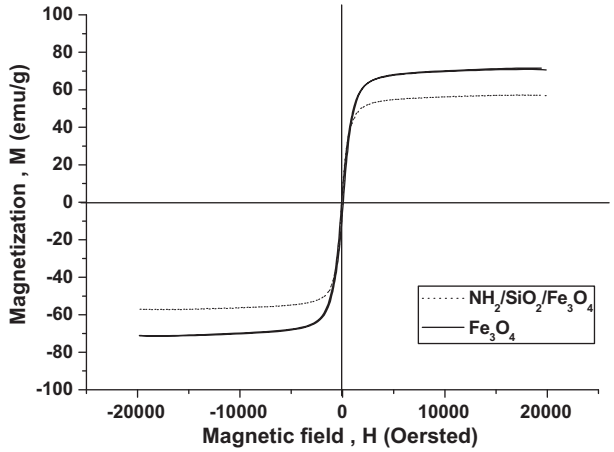

Fig. 5. Magnetization versus applied magnetic field for Fe_3O_4 and $NH_2/SiO_2/Fe_3O_4$.

shell was found to lower the saturation magnetization of magnetite particles [34]. The results in Fig. 5 also indicated that the prepared particles exhibited a paramagnetic behavior at room temperature [35,36].

3.2. Effect of pH on adsorption of copper ions and RB5

Fig. 6 shows the performance of the $NH_2/SiO_2/Fe_3O_4$ adsorbent in adsorbing copper ions and RB5 at different solution pH values, and reveals that the adsorption behavior of $NH_2/SiO_2/Fe_3O_4$ with Cu^{2+} and RB5 is strongly pH-dependent. The amine groups ($-NH_2$) of $NH_2/SiO_2/Fe_3O_4$ will be protonated (NH_3^+) or not depending on the pH values of the solution. The amine forms of NH_3^+ and NH_2 will attract anions [37] and cations [38], respectively. At solution pH 3, the adsorption efficiency of Cu^{2+} by $NH_2/SiO_2/Fe_3O_4$ was nearly zero, but for RB5, it was the highest. At low solution pH values, a relatively high concentration of protons would strongly compete with copper ions for amine sites, so that the adsorption of copper ions was significantly decreased. Furthermore, the protonation of the amine groups would lead to strong electrostatic repulsion of the copper ions to be adsorbed. As a result, it became difficult for the copper ions to come into close contact with the adsorbent surface and be adsorbed on it; this resulted in poor adsorption performance for Cu^{2+} at solution pH $\leqq$3. On the other hand, the protonated amines possess a strong electrostatic attraction to RB5, which leads to a high adsorption capacity. For RB5 adsorption, the optimum pH is 3. The adsorption capacity decreased when the solution pH was below 3, which may be attributed to the fact that the anionic groups and sulfonate groups were surrounded by protons, which inhibited the attraction between the amine adsorbent and the azo dyes.

At higher solution pH values of 4–6 (lower proton concentrations), as regards the copper ions, the competition between protons and copper ions for the amine groups became less significant, and more of the amine groups existed in their neutral form, which reduced the electrostatic repulsion of the copper ions. Furthermore, the unpaired electrons of the amine groups could also create coordinate bonds with the copper ions. More copper ions could thus be adsorbed onto the surfaces of $NH_2/SiO_2/Fe_3O_4$, resulting in the observed increase in Cu^{2+} adsorption on the adsorbent. With regard to RB5, at higher solution pH, less protons will be available to protonate the amine groups ($-NH_2$) of $NH_2/SiO_2/Fe_3O_4$ to form NH_3^+, thereby decreasing the electrostatic attractions between negatively charged dye anions [37]; this decrease is attributed to the lower degree of adsorption.

Fig. 6 indicates the complete removal of Cu^{2+} from the solution when the solution pH value exceeded 6.5. This took place because Cu^{2+} began to precipitate as $Cu(OH)_2$. Therefore, copper ions were removed by both adsorption and precipitation when the solution pH value exceeded 6.5 [39]. With increasing solution pH, the quantity of protonic amine groups decreased, which is attributed to the lower adsorption capacity of the amine magnetic adsorbent in relation to RB5.

As a result, the optimum pH values for Cu^{2+} and RB5 adsorption were found to be in the pH range of 5–6 and 3, respectively, and all further adsorption experiments were carried out at solution pH 5.5 for Cu^{2+}, and pH 3 for RB5.

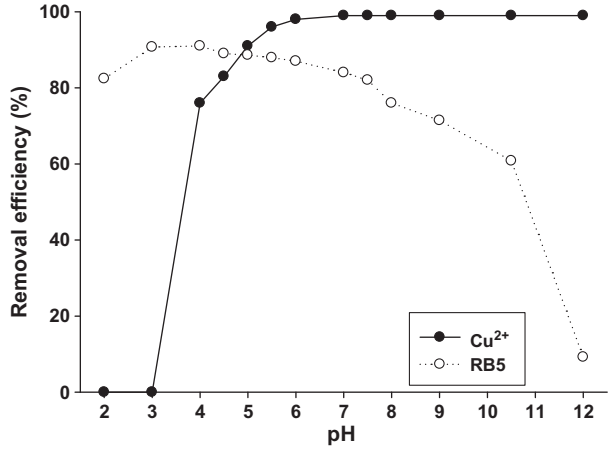

Fig. 6. Effect of solution pH values on copper ion adsorption on the $NH_2/SiO_2/Fe_3O_4$ adsorbent. Experimental conditions: initial concentrations of Cu^{2+} and RB5 were 100 mg L^{-1} and 500 mg L^{-1}, respectively, $NH_2/SiO_2/Fe_3O_4$ 10 g L^{-1}, reaction time = 24 h, temperature (T) = 298 K. The pH value of the solution was controlled by adding 0.1 N HNO_3/NaOH.

3.3. Adsorption isotherms of copper ions and RB5

Adsorption isotherms indicate how the adsorbates, Cu^{2+} and RB5, interact with adsorbents and how adsorption uptakes vary with adsorbate concentrations at given pH values and temperatures. The data equilibrium isotherms for the adsorption of copper ions and RB5 by $NH_2/SiO_2/Fe_3O_4$ are listed in Table 2, and they are fitted by Langmuir and Freundlich isotherm equations [40,41]. The

Table 2
Adsorption isotherm results for copper ion and RB5 adsorption on the $NH_2/SiO_2/Fe_3O_4$ adsorbents at solution pH value = 5.5 for Cu^{2+} (A), and pH value = 3.0 for RB5 (B), $NH_2/SiO_2/Fe_3O_4$ 10 g L^{-1}, reaction time = 24 h, temperature (T) = 298 K.

Initial concentration Cu^{2+} (mg L^{-1})	Equilibrium concentration (Ce, mg L^{-1})	Adsorption quantity (mg g^{-1})
(A)		
25	1.21	2.38
50	3.39	4.66
75	6.12	6.89
100	19.06	8.09
125	34.76	9.02
Initial concentration RB5 (mg L^{-1})	Equilibrium concentration (Ce, mg L^{-1})	Adsorption quantity (mg g^{-1})
(B)		
500	40	115
600	55	136
700	92	152
800	126	169
900	192	177
1000	207	198

Table 3
Parameter values of the different types of adsorption isotherm models fitting to the experimental results in Table 2 for copper ion and RB5, respectively, adsorption on the $NH_2/SiO_2/Fe_3O_4$ adsorbents.

	Langmuir			Freundlich		
	Q_m (mg g^{-1})	K_L (L mg^{-1})	R^2	n	K_F	R^2
Cu^{2+}	10.41	0.0376	0.9956	2.63	1.53	0.8906
RB5	217	0.000744	0.9711	3.47	5.03	0.9596

Langmuir equation can be expressed as follows:

$$\frac{C_e}{q_e} = \frac{C_e}{q_m} + \frac{1}{q_m K_L} \quad (1)$$

where q_e is the equilibrium adsorption capacity of copper ions on the adsorbent (mg g^{-1}); C_e, the equilibrium copper ion concentration in solution (mg L^{-1}); q_m, the maximum capacity of the adsorbent (mg g^{-1}); and K_L, the Langmuir adsorption constant (L mg^{-1}). The linear form of a Freundlich equation can be represented as follows:

$$\log q_e = \log K_F + \frac{1}{n} \log C_e \quad (2)$$

where q_e and C_e are defined as above, K_F is the Freundlich constant (L mg^{-1}), and n is the heterogeneity factor.

Table 3 lists the values of q_m and K_L, as determined from the slope and intercept of the linear plots of C_e/q_e versus C_e, and the values of K_F and $1/n$, as determined from the slope and intercept of the linear plot of ln q_e versus ln C_e. The resulting correlation coefficients listed in Table 3 reveal that the data were fitted better by the Langmuir equation than by the Freundlich equation for both Cu^{2+} and RB5. Fitting of the Langmuir isotherm indicates monolayer coverage of these two adsorbates on the surface of $NH_2/SiO_2/Fe_3O_4$ during adsorption. The maximum monolayer copper uptake (q_m) was found to be 10.41 mg g^{-1} for Cu^{2+} and 217 mg g^{-1} for RB5.

3.4. Adsorption kinetics

Fig. 7 shows the effect of contact time on the adsorption of Cu^{2+} and RB5 by $NH_2/SiO_2/Fe_3O_4$ from a solution at a temperature of 25 °C. The term C/C_0 on the vertical axis of Fig. 7 denotes residual concentration versus initial concentration of the target compounds. The adsorption occurred rapidly during the early stages of the adsorption reaction for both Cu^{2+} and RB5, which was probably due to the abundant availability of active sites on the adsorbents. However, with a gradual decrease in the number of active sites in the bulk solution, the adsorption reaction became slower. The adsorption of Cu^{2+} and RB5 at other temperatures, i.e., 40 °C and 55 °C, revealed phenomena similar to those at 25 °C.

Adsorption kinetic data are often analyzed using two commonly used kinetic models, namely, the pseudo-first-order and pseudo-second-order kinetic models, which can be expressed in their linearized forms as Eqs. (3) and (4), respectively [42]:

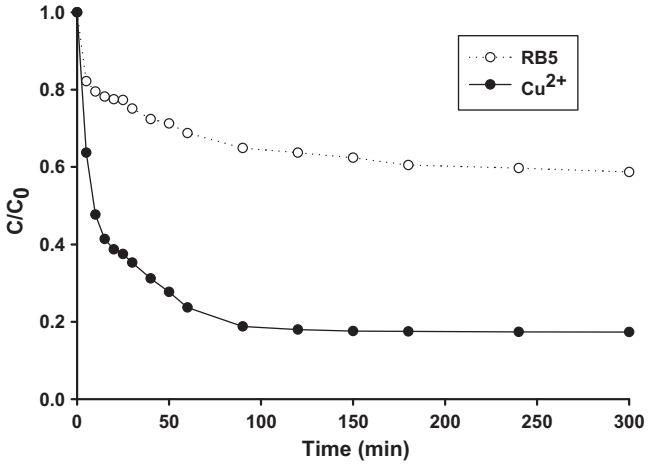

Fig. 7. Dependence of adsorption of Cu^{2+} and RB5 by $NH_2/SiO_2/Fe_3O_4$ on time at 298 K. Experimental conditions: $C_{RB5,0}$ = 500 mg L^{-1}, $NH_2/SiO_2/Fe_3O_4$ 10 g L^{-1}, pH 5.5 for Cu^{2+}, pH 3 for RB5. The pH value of the solution was controlled by adding 0.1 N HNO_3/NaOH.

$$\log(q_e - q_t) = \log q_e - \frac{k_1}{2.303} t \quad (3)$$

$$\frac{t}{q_t} = \frac{1}{k_2 q_e^2} + \frac{1}{q_e} t \quad (4)$$

where q_t (mg g^{-1}) is the adsorption uptake at time t (min); q_e (mg g^{-1}) is the adsorption capacity at adsorption equilibrium; and k_1 (min^{-1}) and k_2 (g mg^{-1} min^{-1}) are the kinetic rate constants for the pseudo-first-order and the pseudo-second-order models, respectively. The adsorption kinetic data at different temperatures were fitted to Eqs. (3) and (4), and the calculated model parameters are listed in Table 4. The results (the correlation coefficients R^2 listed in Table 4) clearly indicate that the adsorption kinetics closely followed the pseudo-second-order kinetic model rather than the pseudo-first-order kinetic model, which suggests that the adsorption process was quite rapid and was probably dominated by a chemical adsorption phenomenon. Moreover, the temperature dependence of the kinetic parameter k_2 in Table 4 can be described by the Arrhenius equation (Eq. (5)).

$$\ln k = \ln A - \frac{E_a}{RT} \quad (5)$$

where A, E_a, T, and R are the frequency factor, activation energy, temperature (K), and gas constant, respectively. By plotting ln k_2 against $1/T$ (1/K), the reaction temperatures are determined to be 298 K, 313 K, and 328 K, which give E_a values of 26.92 kJ mol^{-1} for Cu^{2+} and 12.06 kJ mol^{-1} for RB5.

Table 4
Parameter values of the kinetics models fitting to the experimental results in Fig. 7 for copper ions and RB5 adsorption on the $NH_2/SiO_2/Fe_3O_4$ adsorbent.

Treatments		R^2		Rate constants	Activated energy
		1st order	2nd order	k_2 (g mg^{-1} min^{-1})	E_a (kJ mol^{-1})
Temperature Cu^{2+}	25 °C	0.964	0.991	0.0010	26.92
	40 °C	0.976	0.996	0.0018	
	55 °C	0.882	0.994	0.0029	
Temperature RB5	25 °C	0.981	0.997	0.000484	12.06
	40 °C	0.948	0.997	0.000598	
	55 °C	0.788	0.995	0.000756	

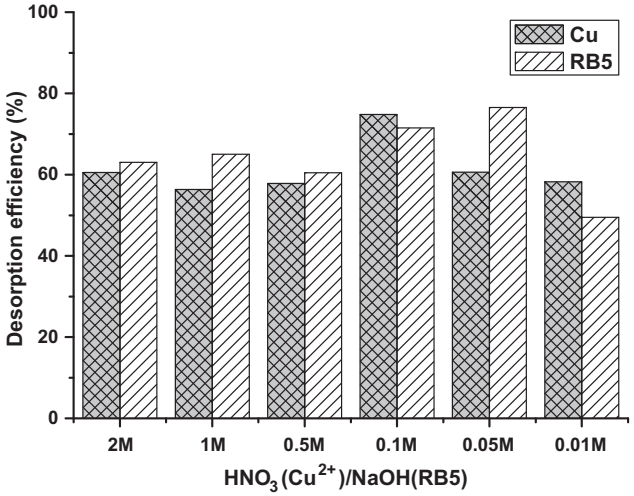

Fig. 8. Desorption efficiency of copper ions and RB5 from the $NH_2/SiO_2/Fe_3O_4$ adsorbent in solutions with different HNO_3 (for Cu^{2+})/NaOH (for RB5) concentrations. Experimental conditions: $NH_2/SiO_2/Fe_3O_4$ 5 g L^{-1}, reaction time = 24 h, T = 298 K.

3.5. Desorption and repeated use

Good desorption performance of an adsorbent is an important factor necessary for its potential practical application. The results shown in Fig. 6 reveal that the $NH_2/SiO_2/Fe_3O_4$ adsorbent did not significantly adsorb copper ions or RB5 at pH < 3 or pH > 10, respectively, which suggests that the adsorbed copper ions and RB5 could possibly be desorbed in a solution with such pH values. Therefore, HNO_3 and NaOH solutions with different concentrations were examined in a desorption study. Fig. 8 shows the desorption efficiency obtained at various HNO_3/NaOH concentrations in desorption solutions. It is interesting to note that the maximum desorption efficiency was achieved at an HNO_3 concentration of 0.1 M, and any higher or lower HNO_3 concentrations resulted in lower desorption efficiencies. In order to explain this, one may assume that the reactions taking place in acidic desorption solutions can be given by the following equations [43]:

$$SiO_2/Fe_3O_4 - NH_2\cdots Cu^{2+} + H^+ \Leftrightarrow SiO_2/Fe_3O_4 - NH_3^+ + Cu^{2+} \quad (6)$$

$$SiO_2/Fe_3O_4 - NH_2 + H^+ \Leftrightarrow SiO_2/Fe_3O_4 - NH_3^+ \quad (7)$$

In a solution with an HNO_3 concentration that exceeds 0.1 M, the high concentration of H^+ will shift both Eqs. (6) and (7) toward the right-hand side and more $SiO_2/Fe_3O_4 - NH_3^+$ will be generated. However, the generation of $SiO_2/Fe_3O_4 - NH_3^+$ will favor the reverse reaction of Eq. (6) to the left-hand side, thus hindering the desorption of copper ions from an adsorbent. Therefore, when the concentration of HNO_3 in the desorption solution exceeded 0.1 M, the reverse reaction in Eq. (6) actually began to hinder the desorption of copper ions from the adsorbents, resulting in reduced desorption efficiency. On the other hand, a concentration lower than 0.1 M HNO_3 (lower H^+ concentration) in the desorption solution may be insufficient to drive the reaction in Eq. (6) to the right-hand side for the desorption of copper ions, thus leading to the observed desorption efficiencies that were lower than that at a 0.1 M HNO_3 concentration.

With regard to RB5 desorption, it is also interesting to note that the maximum desorption efficiency was achieved at an NaOH concentration of 0.05 M, and any higher or lower NaOH concentrations resulted in lower desorption efficiencies. The reason for this is similar to the former explanation of Cu^{2+} desorption from a magnetic adsorbent. In a solution with an NaOH concentration that exceeds 0.05 M, the high concentration of OH^- will shift both Eqs. (8) and (9) toward the right-hand side and more $SiO_2/Fe_3O_4 - NH_2$ will be generated. However, the generation of $SiO_2/Fe_3O_4 - NH_2$ will favor the reverse reaction of Eq. (9) to the left-hand side, thus hindering the desorption of RB5from an adsorbent.

$$SiO_2/Fe_3O_4{-}NH_3^+\cdots RB5 + OH^- \Leftrightarrow SiO_2/Fe_3O_4 - NH_2 + RB5 + H_2O \quad (8)$$

$$SiO_2/Fe_3O_4 - NH_3^+ + OH^- \Leftrightarrow SiO_2/Fe_3O_4 - NH_2 + H_2O \quad (9)$$

In order to determine the reusability of $NH_2/SiO_2/Fe_3O_4$, adsorption–desorption cycles were repeated three times using the same amine magnetic adsorbent. The adsorption capacity for Cu^{2+} and RB5 of the recycled $NH_2/SiO_2/Fe_3O_4$ exhibited a loss of approximately 13.6% and 15.7%, respectively, in the third cycle.

4. Conclusions

Amine-functionalized silica magnetite, $NH_2/SiO_2/Fe_3O_4$, has been synthesized using TPED as the surface modification agent; TPED behaves as an anionic or cationic adsorbent depending on the pH value of the aqueous solution, making the amino groups protonic or neutral, respectively. In a batch system, the optimum solution pH for Cu^{2+} and RB5 adsorption by $NH_2/SiO_2/Fe_3O_4$ was found to be 5.5 and 3, respectively. The adsorption behavior of Cu^{2+} and RB5 adsorption by $NH_2/SiO_2/Fe_3O_4$ were in good agreement with the Langmuir adsorption isotherm, and the maximum adsorption capacity (q_m) of Cu^{2+} and RB5 were 10.41 mg g^{-1} and 217 mg g^{-1}, respectively. Since magnetic adsorbent is a potential water treatment method, the results of this study will be helpful in the development of amino-group-containing magnetic adsorbents that can be used to remove anionic and cationic groups in aqueous solution.

References

[1] Y. Nuhoglu, E. Oguz, Removal of copper(II) from aqueous solutions by biosorption on the cone biomass of *Thuja orientalis*, Proc. Biochem. 38 (2003) 1627–1631.
[2] S.J. Pollack, I.I.J. Sadler, S.R. Hawtin, V.J. Tailor, M.S. Shearman, Sulfonated dyes attenuate the toxic effects of β-amyloid in a structure-specific fashion, Neurosci. Lett. 197 (1995) 211–214.
[3] F. Ekmekyapar, A. Aslan, Y. Kemal Bayhan, A. Cakici, Biosorption of copper(II) by nonliving lichen biomass of Cladonia rangiformis hoffm, J. Hazard. Mater. B 137 (2006) 293–298.
[4] A. Szyguła, E. Guibal, M. Ruiz, A.M. Sastre, The removal of sulphonated azo-dyes by coagulation with chitosan, Colloids Surf. A: Physicochem. Eng. Aspects 330 (2008) 219–226.
[5] E. Forgacs, T. Cserhati, G. Oros, Removal of synthetic dyes from waste waters: a review, Environ. Int. 30 (2004) 953–971.
[6] G. Crini, Non-conventional low-cost adsorbents for dye removal: a review, Bioresour. Technol. 97 (2006) (2006) 1061–1085.
[7] S. Al-Degs Yahya, I. El-Barghouthi Musa, H. El-Sheikh Amjad, M. Walker Gavin, Effect of solution pH, ionic strength, and temperature on adsorption behavior of reactive dyes on activated carbon, Dyes Pigments 77 (2008) 16–23.
[8] A.K. Jain, V.K. Gupta, A. Bhatnagar, Suhas, Utilization of industrial waste products as adsorbents for the removal of dyes, J. Hazard. Mater. 101 (2003) 31–42.
[9] M. Prasad, S. Saxena, Sorption mechanism of some divalent metal ions onto low-cost mineral adsorbent, Ind. Eng. Chem. Res. 43 (2004) 1512–1522.
[10] C.C. Liu, M.K. Wang, Y.S. Li, Removal of nickel from aqueous solution using wine processing waste sludge, Ind. Eng. Chem. Res. 44 (2005) 1438–1445.
[11] N. Li, R.B. Bai, C. Liu, Enhanced and selective adsorption of mercury ions on chitosan beads grafted with polyacrylamide via surface-initiated atom transfer radical polymerization, Langmuir 21 (2005) 11780–11787.
[12] N. Li, R.B. Bai, Copper adsorption on chitosan–cellulose hydrogel beads: behaviors and mechanisms, Sep. Purif. Technol. 42 (2005) 237–247.
[13] M. Ghoul, M. Bacquet, M. Morcellet, Uptake of heavy metals from synthetic aqueous solutions using modified PEI-silica gels, Water Res. 37 (2003) 729–734.
[14] R.K. Gupta, R.A. Singh, S.S. Dubey, Removal of mercury ions from aqueous solutions by composite of polyaniline with polystyrene, Sep. Purif. Technol. 38 (2004) 225–232.
[15] M. Chanda, G.L. Rempel, Polyethyleneimine gel-coat on silica: high uranium capacity and fast kinetics of gel-coated resin, React. Polym. 25 (1995) 25–36.

[16] C.S. Chiou, J.S. Shih, Bifunctional cryptand modifier for capillary electrophoresis in separation of inorganic/organic anions and inorganic cations, Analyst 121 (1996) 1107–1110 (SCI).
[17] L. Jin, R.B. Bai, Mechanisms of lead adsorption on chitosan/PVA hydrogel beads, Langmuir 18 (2002) 9765–9770.
[18] A.A. Atia, A.M. Donia, S.A. Abou-El-Enein, A.M. Yousif, Studies on uptake behavior of copper(II) and lead(II) by amine chelating resins with different textural properties, Sep. Purif. Technol. 33 (2003) 295–301.
[19] G. Bayramoglu, M.Y. Arica, Ethylenediamine grafted poly (glycidyl-methacrylate-co-methylmethacrylate) adsorbent for removal of chromate anions, Sep. Purif. Technol. 45 (2005) 192–199.
[20] W. Yantasee, Y. Lin, G.E. Fryxell, K.L. Alford, B.J. Busche, C.D. Johnson, Selective removal of copper(II) from aqueous solutions using fine-grained activated carbon functionalized with amine, Ind. Eng. Chem. Res. 43 (2004) 2759–2764.
[21] S. Deng, R.B. Bai, J.P. Chen, Aminated polyacrylonitrile fibers for lead and copper removal, Langmuir 19 (2003) 5058–5064.
[22] J. Hu, G. Chen, I.M.C. Lo, Removal and recovery of Cr(VI) from wastewater by maghemite nanoparticles, Water Res. 39 (2005) 4528–4536.
[23] C. Albornoz, E.E. Sileo, S.E. Jacobo, Magnetic polymers of maghemite (g-Fe_2O_3) and polyvinyl alcohol, Physica B 354 (2004) 149–153.
[24] H.W. Chen, Y.L. Kuo, C.S. Chiou, S.W. You, C.M. Ma, C.T. Chang, Mineralization of Reactive Black 5 in Aqueous solution by ozone/H_2O_2 in the presence of a magnetic catalyst, J. Hazard. Mater. 174 (2010) 795–800.
[25] M.D. Butterworth, L. Illum, S.S. Davis, Preparation of ultrafine silica- and PEG-coated magnetite particles, Colloids Surf. A: Physicochem. Eng. Aspects 179 (2001) 93–102.
[26] X. Liu, Z. Ma, J. Xing, H. Liu, Preparation and characterization of amino–silane modified superparamagnetic silica nanospheres, J. Magn. Magn. Mater. 270 (2004) 1–6.
[27] N.T.S. Phan, C.W. Jones, Highly accessible catalytic sites on recyclable organosilane-functionalized magnetic nanoparticles: an alternative to functionalized porous silica catalysts, J. Mol. Catal. A: Chem. 253 (2006) 123–131.
[28] C.F. Chang, C.Y. Chang, T.L. Hsu, Preparation and adsorptive application of novel superparamagnetic zirconia material, Colloids Surf. A: Physicochem. Eng. Aspects 327 (2008) 64–70.
[29] R.K. Iler, The Chemistry of Silica, John Wiley & Sons, New York, 1979.
[30] A.G.S. Prado, J.A.A. Sales, R.M. Carvalho, J.C. Rubim, C. Airoldi, Immobilization of 5-amino-1, 3,4-thiadiazole-thiol onto silica gel surface by heterogeneous and homogeneous routes, J. Non-Cryst. Solids 333 (2004) 61–67.
[31] M. Aslam, L. Fu, S. Li, V.P. Dravid, Silica encapsulation and magnetic properties of FePt nanoparticles, J. Colloid. Interface Sci. 290 (2005) 444–449.
[32] A. Campo, T. Sena, J.P. Lellouchec, I.J. Bruce, Multifunctional magnetite and silica–magnetite nanoparticles: synthesis, surface activation and applications in life sciences, J. Magn. Magn. Mater. 293 (2005) 33–40.
[33] Y.L. Shi, W.Q.Y. Zheng, Synthesis and characterization of a POM-based nanocomposite as a novel magnetic photocatalyst, J. Phys. Chem. Solids 67 (2006) 2409–2418.
[34] C.R. Vestal, Z.J. Zhang, Atom transfer radical polymerization synthesis and magnetic characterization of $MnFe_2O_4$/polystyrene core/shell nanoparticles, J. Am. Chem. Soc. 124 (2002) 14312–14313.
[35] J. Xu, Y. Ao, D. Fu, C. Yuan, Low-temperature preparation of anatase titania-coated magnetite, J. Phys. Chem. Solids 69 (2008) 1980–1984.
[36] Q.A. Pankhurst, J. Connolly, S.K. Jones, J. Dobson, Application of magnetic nanoparticles in biomedicine, J. Phys. D 36 (2003) R167–R181.
[37] G. Annadurai, L.Y. Ling, J.F. Lee, Adsorption of reactive dye from an aqueous solution by chitosan: isotherm, kinetic and thermodynamic analysis, J. Hazard. Mater. 152 (2008) 337–346.
[38] S.S. Banerjee, D.H. Chen, Fast removal of copper ions by gum Arabic modified magnetic nano-adsorbent, J. Hazard. Mater. 147 (2007) 792–799.
[39] D.C.K. Ko, J.F. Porter, G. McKay, Mass transport model for the fixed bed sorption of metal ions on bone char, Ind. Eng. Chem. Res. 42 (2003) 3458–3469.
[40] Y.C. Wong, Y.S. Szeto, W.H. Cheung, G. Mckay, Equilibrium studies for acid dye adsorption onto chitosan, Langmuir 19 (2003) 7888–7894.
[41] Y.S. Ho, G. McKay, Kinetic models for the sorption of dye from aqueous solution by wood, Trans. Inst. Chem. Eng. 76B (1998) 183–191.
[42] A. Mellah, S. Chegrouche, M. Barkat, The removal of uranium(VI) from aqueous solutions onto activated carbon: kinetic and thermodynamic investigations, J. Colloid Interface Sci. 296 (2006) 434–441.
[43] C.K. Liu, R. Bai, L. Hong, Diethylenetriamine-grafted poly(glycidyl methacrylate) adsorbent for effective copper ion adsorption, J. Colloid Interface Sci. 303 (2006) 99–108.